Graphene-Metal Oxide Based Nanocomposites for Supercapacitor Applications

D. Selvakumar, P. Nagaraju, R. Jayavel

Centre for Nanoscience and Technology, Anna University, Chennai -600 025, India, rjvel@annauniv.edu

ABSTRACT

In this work graphene/TiO_2, WO_3 nanocomposites were synthesized by facile, surfactant free, *in-situ* microwave irradiation method, a quick but also are eco-friendly approach. The structure, morphology, composition and thermal stability of the composites were characterized by using XRD, SEM, Raman spectroscopy, and XPS analyses. The SEM and HR-TEM analyses demonstrate the spherical TiO_2 and WO_3 nanoparticles intercalated on the graphene sheets. XPS studies confirm the binding states of the composite structure. The nanocomposites used as the supercapacitor electrode in three electrode system exhibited higher specific capacitance. The enhanced capacitive performance is due to the intercalation of TiO_2 and WO_3 nanoparticles on the graphene sheet. The *in-situ* microwave irradiation method brings a viable, low-cost and facile synthesis of different metal oxide/graphene based composites with promising properties as supercapacitors for energy storage applications.

Key words: graphene oxide, microwave irradiation supercapacitor.

1. INTRODUCTION

Rapid increase in industrialization has led to a number of severe problems, which in-turn might have a major social impact on issues such as increased usage of electronic devices, large memory back-up devices, renewable-energy power plants and electronic vehicles. This increased usage leads to an enhanced demand for energy storage devices. The need for the development of materials for electrochemical storage with improved performance has become an urgent requirement. Supercapacitors with their unique properties such as fast charging–discharging, high power density and long cycle life time are complementary to rechargeable batteries [1, 2].

Recent research is focused mainly on the development of supercapacitor with combined electrode containing redox active materials and porous carbon materials for achieving both high power and energy density [3]. Till date, the ever increasing growth of research activities in nanoscience and nanotechnology continually brings out new physical and chemical properties of TiO_2 and WO_3 nanomaterials and thus provides new opportunity for the growth of TiO_2 and WO_3 based wide-band gap semiconductor material for varied applications. TiO_2 and WO_3 have been studied for application in large scale energy storage owing to their high specific capacity and high current rate tolerance with various morphologies [4]. Conductive coating and/or adding conductive mediators were developed in order to improve the electronic conductivity of TiO_2, WO_3 nanoparticles [5, 6].

In recent years, various classes of carbon-based materials are being explored. Among them, graphene has emerged as one of the most interesting materials for supercapacitor applications. Incorporation of TiO_2 and WO_3 into conductive graphene electrode overcomes the drawbacks in the conductivity and mechanical flexibility of either graphene or TiO_2/WO_3 electrode. Hence, TiO_2 and WO_3 were used as additives to carbon materials, especially graphene for enhanced performance.

Recently, several attempts to synthesize TiO_2 and WO_3 /graphene nanocomposites by different methods have been reported in order to fabricate suitable electrode material for supercapacitors applications. An eco-friendly and facile approach for the synthesis of TiO_2 and WO_3 /graphene is essential. Microwave irradiation synthesis is one of the most popular techniques adapted in industries as well as in domestic applications due to the efficient and fast transfer of energy and influence on the size, shape and morphology of the prepared material [7, 8]. In the present work, TiO_2 and WO_3 /graphene nanocomposites were synthesized by facile *in-situ* microwave irradiation method. In this method, homogeneous distribution of TiO_2 and WO_3 nanoparticles on to the graphene sheet and simultaneous reduction of graphene oxide to graphene were achieved via microwave irradiation. This method enhances the specific surface area and the supercapacitor performance.

2. EXPERIMENTAL

2.1 Formation of TiO_2/WO_3 /Graphene nanocomposite

Graphene oxide was synthesized by the modified Hummer's method [9]. The TiO_2 and WO_3/graphene nanocomposites were synthesized by the facile *in-situ* microwave irradiation method. Initially 60 mg of graphene oxide was added to 60 ml of DI water and treated ultrasonically for about 1 h. Titanium (IV) n-butoxide (0.1 M) /sodium tungstate was added to graphene oxide solution followed by stirring for 1 h. The above mixed solution was kept in the microwave oven at 850W for 10 min. The reaction mixture was then allowed to cool down to room temperature and 2 ml of the reducing agent (H_6N_2O) was added and stirred for 2 h. The solution was kept in the microwave oven under the same conditions as mentioned above. Finally, the grayish-black product was collected, indicating the reduction of graphene oxide into the graphene. The final product was

 TechConnect Briefs 2018, TechConnect.org, ISBN 978-0-9988782-2-5

filtered and washed using ethanol, water for several times and dried in vacuum oven at 60 °C for 12 h. The above protocol was followed for the synthesis of pure TiO_2 and WO_3 nanoparticles and graphene separately.

2.2 Electrochemical studies

The electrochemical performance of the nanocomposites was investigated by Chronopotentiometry (CP) analysis. For the preparation of working electrode, TiO_2, WO_3 /graphene nanocomposite, ethanol and nafion solution were mixed homogeneously. The prepared material was coated onto the glassy carbon electrode and allowed to dry for a few minutes. Cyclic voltammetry (CV) measurements were carried out in 1 M H_2SO_4, Na_2SO_4 electrolyte (vs. Ag/AgCl) at different scan rates from 5 to 100 mVs^{-1}. The mass loading of the electrode active material was 3 mg. All electrochemical studies were performed at room atmospheric condition.

3. RESULTS AND DISCUSSION

Fig. 1 (a) shows the powder XRD pattern of synthesized graphene. XRD pattern of graphene with prominent (002) peak. The diffraction peaks match with the standard pattern (JCPDF NO: 75-1621) and confirmed the hexagonal phase of the graphene. XRD patterns of pure TiO_2 and TiO_2/graphene composite are shown in Fig. 1 (a). For TiO_2, the tetragonal anatase phase is in good agreement with (JCPDS NO: 211272). The characteristic peak of graphene (002) peak is not observed in the XRD pattern due to the overlapping with (101) peak of TiO_2 and low amount of graphene used for the composite formation [10]. The microwave reaction results in crystalline tungstic acid hydrates ($WO_3.H_2O$) as shown in Fig. 1 (b) and well matched with the JCPDS card No. 48-0719 [11]. Fig. 1(b) indicates the diffraction peaks correspond to the monoclinic phase of WO_3 (JCPDS: 43-1035) after calcining at 500°C. Fig. 2(d) depicts the diffraction pattern of WO_3/G composite, which is almost similar to the crystalline phase of WO_3 with reduced intensity. No diffraction peaks of graphene were observed in the TiO_2, WO_3/G composite due to the disordered structure formed by the contact between WO_3 and graphene sheet with relatively low intensity of graphene than WO_3 [9, 12].

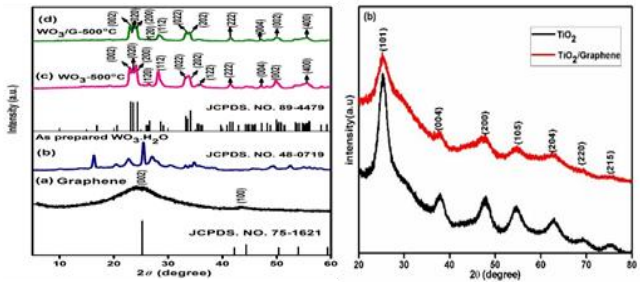

Fig. 1. XRD patterns of (a) TiO_2/graphene and (b) WO_3/graphene composites.

The high resolution transmission electron microscope (HR-TEM) images of the nanocomposite reveals the uniform decoration of TiO_2 and WO_3 on the graphene sheets as shown in Fig. 2 (a, c) . The sheet like structure of graphene decorated TiO_2 and WO_3 nanoparticles controls the aggregation and hence increases the specific surface area. The crystalline nature of TiO_2 nanoparticles was confirmed by lattice fringes with clear d-spacing. Fig. 2 (b) shows the inter-planar lattice spacing of 0.35 nm, which corresponds to the (101) plane of the anatase phase of TiO_2[13]. Inset in Fig. 2 (c) illustrates the fast Fourier transform (FFT) image of TiO_2/graphene composite. Fig. 2(d) shows the lattice-fringe pattern with an inter-planar spacing of 0.32 nm corresponding to the (002) plane of the monoclinic WO_3 lattice. The inter-planar spacing of graphene (0.37 nm) is higher than that of graphite (0.34 nm) and lower than graphene oxide (0.83 nm).

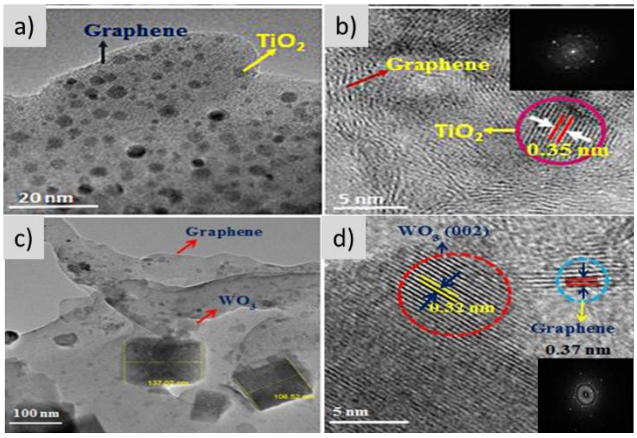

Fig. 2. HR-TEM images of (a, c) TiO_2, WO_3 /graphene nanocomposite. Insets in Fig. 2(b, d) show the FFT pattern of the composite.

Raman spectra shown in Fig. 3 (a) exhibits two peaks at 1334 (D band) and 1579 cm^{-1} (G band). For TiO_2, three strong vibrational peaks are located at 402, 513 and 640 cm^{-1} corresponding to B_1g, B_1g A_1g^+, and Eg modes of anatase phase [14]. In TiO_2/graphene nanocomposite, TiO_2 characteristic peaks are observed along with graphene peaks at 1325 and 1596 cm^{-1}. The D/G ratio of graphene oxide and TiO_2/graphene composite are 0.809 and 0.865 respectively. The TiO_2/graphene composite shows an increased D/G intensity ratio compared to graphene oxide. This confirms the decrease in the average size of the in-plane sp^2 domains due to the reduction of the exfoliated graphene oxide, due to the presence of graphene in the TiO_2/graphene composite [15].

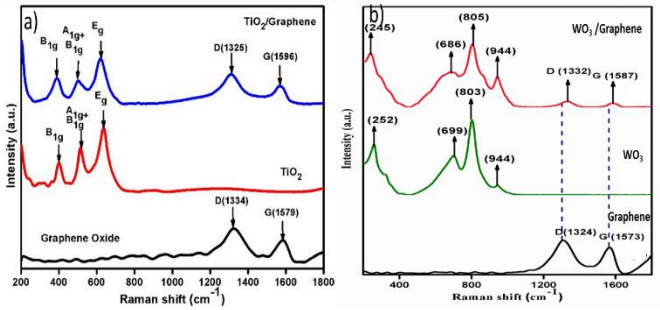

Fig. 3. Raman spectra of (a) TiO_2 and (b) WO_3 based graphene nanocomposite.

Fig. 3 (b) shows the WO_3 electrode bands at around 803 cm^{-1} and 699 cm^{-1} corresponding to the O–W–O stretching modes, which are the strong characteristic peaks of WO_3 crystallites. Additionally, the peak at 252 cm^{-1} is related to the W–O–W bending mode and 944 cm^{-1} is attributed to the symmetric mode of terminal W^{6+}=O bond. The D and G bands observed for the WO_3/G nanocomposite with less intensity reveal the formation of composite structure. The peak at 699 cm^{-1} due to W=O bond was broadened and shifted to 686 cm^{-1} in the WO_3/G, probably due to the formation of C–O–W bonds between the graphene and WO_3 nanoplates [16, 17].

The XPS spectra of TiO_2 and WO_3 /graphene nanocomposites are shown in Fig. 4. The survey spectrum (Fig. 4 (a)) of the TiO_2/graphene showed peaks of Ti, C and O confirming the presence of all elements in the composite. The Ti-2p core-level photoelectron spectrum reveals Ti $2p_{3/2}$ (458.5 eV) and Ti $2p_{1/2}$ (465.4 eV), which agree with the binding energy values of pure anatase Ti^{4+}.

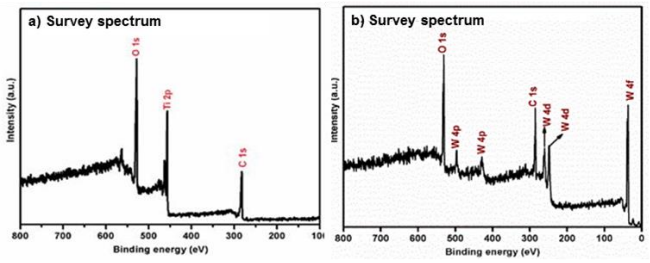

Fig. 4. XPS survey spectra of (a) TiO_2/graphene (b) WO_3/ graphene nanocomposite.

The deconvoluted spectrum of Ti 2p shown in Fig. 4 (a) revealed peaks centered at 465.8 and 460.2 eV, associated with the formation of Ti-C bonds in the TiO_2/graphene nanocomposite [18]. Fig. 4(b) represents the XPS of WO_3/G spectra of the W 4f doublet peaks. The binding energy states of W $4f_{7/2}$ and W $4f_{5/2}$ were observed at 37.79 eV and 35.74 eV, respectively. The separation between W $4f_{7/2}$ and W $4f_{5/2}$ core levels was 2.85 eV, indicating the normal state of W^{6+} in the cubic spinel WO_3 structure. The BET studies revealed that the synthesized TiO_2/grapheme, WO_3/G nanocomposites possess specific surface area of 529.99 m^2g^{-1}, 17.55 $m^2g^{-1,}$ suggesting the successful reduction of graphene oxide into graphene and intercalation TiO_2, WO_3 nanoparticles in the graphene sheet.

The electrochemical properties of TiO_2, WO_3 /graphene nanocomposite electrode were systematically analyzed in 1M H_2SO_4, Na_2SO_4 electrolyte by using three electrode system. electrodes. The CP curves of TiO_2 electrode at different current densities in 1M H_2SO_4 electrolyte are shown in Fig. 5 (a) reveal that the electrode has good capacitive behavior with superior electrochemical reversibility. The shape of CP curves, the derivative voltage-time profile and the symmetric charge-discharge curves indicate the non-Faradic redox reaction exhibited by the TiO_2/graphene electrode. Comparison of CP curves of TiO_2, graphene oxide, TiO_2/graphene composite electrodes at a current density of 1 Ag^{-1}. The composite electrodes have higher charge-discharge time than pure TiO_2 and graphene oxide electrodes, which demonstrates that the composite electrode exhibit the highest specific capacitance and excellent electrochemical performance.

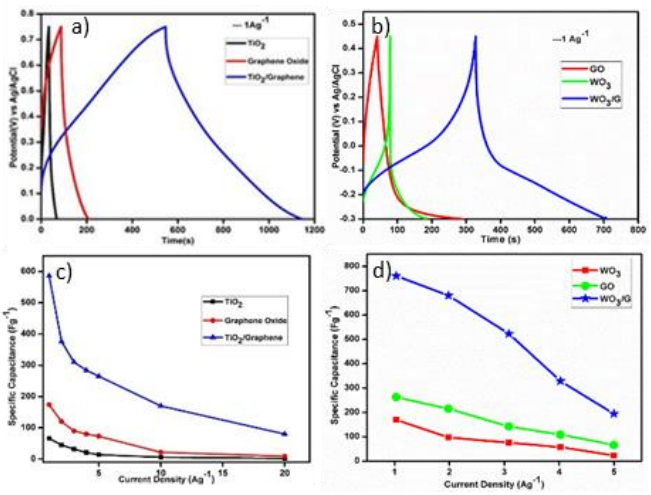

Fig. 5. CP curves and specific capacitance (c) TiO_2 and (d) WO_3 /graphene composite.

The specific capacitance of the TiO_2, WO_3 /graphene electrode was calculated using the equation

$$Cs = I * \Delta t / \Delta V * m \quad (1)$$

where, I-is the constant applied current, Δt-is the discharge time, m-is the mass of the electro-active material and ΔV-is the potential window. For TiO_2 and WO_3 /graphene electrode, the specific capacitance values were calculated to be 585, 761 Fg^{-1} at current densities of $1Ag^{-1}$ respectively. The specific capacitance values were higher than the other electrodes. The decrease in specific capacitance at higher current density may be ascribed to the large portions of the electrode surface that are inaccessible to the electrolyte [19].

The long cyclic stability is the most important requirement for supercapacitor applications. The specific capacitance retention of the TiO_2/graphene, WO_3/graphene electrode reached 100% at 5000 cycles, 100 %, 99.2 % of its initial capacitance, exhibiting good cycl ing stability.

$$\eta = t_d / t_c * 100 \quad (2)$$

where, η-is the Columbic efficiency, t_d and t_c are the discharge and charging time derived from charge–discharge curves. The Columbic efficiency (η) of TiO_2 and WO_3/graphene electrodes were calculated to be 99.8% and 98.2%. Based on the electrochemical analysis, it was concluded that the composite electrode exhibited a higher specific capacitance, good rate capability, and highly efficient for supercapacitor applications.

4. CONCLUSION

The nanocomposites of TiO_2 and WO_3/graphene were synthesized by a facile *in-situ* microwave irradiation method without the assistance of any surfactant. The structure and morphology of the prepared composites were characterized by XRD and SEM analysis. Functional groups and phase formation of the synthesized material were further confirmed by and XPS and Raman spectroscopy studies. Based on the electrochemical studies, the enhanced specific capacitance values of composite electrodes are attributed to the combination of pseudocapacitance of the metal oxides and partially influenced by the inherent double layer capacitance of the graphene sheet. The composite electrode revealed excellent cyclic stability indicating that the nanocomposite can be used as a potential electrode material for supercapacitor applications.

REFERENCES

[1] C. Xiang, M. Li, M. Zhi, A. Manivannan, N. Wu, "Reduced graphene oxide/titanium dioxide composites for supercapacitor electrodes: shape and coupling effects", J. Mater. Chem., 22, 19161, 2012.

[2] H. Xiao, W. Guo, B. Sun, M. Pei, G. Zhou, "Mesoporous TiO_2 and Co-doped TiO_2 Nanotubes/Reduced Graphene Oxide Composites as Electrodes for Supercapacitors", Electrochimi. Acta, 190, 104, 2016.

[3] Y. Chen, X. Zhang, D. Zhang, P. yu, Y. Ma, "High performance supercapacitors based on reduced graphene oxide in aqueous and ionic liquid electrolytes", Carbon, 49, 573, 2011.

[4] R. Liu, W. Guo, B. Sun, J. Pang, M. Pei, G. Zhou, "Composites of rutile TiO_2 nanorods loaded on graphene oxide nanosheet with enhanced electrochemical performance", Electrochim. Acta, 156, 274, 2015.

[5] D. Deng, M.G. Kim, J.Y. Lee, J. Cho, "Green energy storage materials: Nanostructured TiO_2 and Sn-based anodes for lithium-ion batteries", Energy & Environ. Sci., 2, 818, 2009.

[6] L. Liang, J. Zhang, Y. Zhou, J. Xie, X. Zhang, M. Guan, B. Pan, Y. Xie, "High-performance flexible electrochromic device based on facile semiconductor-to-metal transition realized by WO(3)·2H(2)O ultrathin nanosheets", Sci. Rep., 3, 1936, 2013.

[7] Z. Tan, G. Chen, Y. Zhu, "Carbon-Based Supercapacitors Produced by the Activation of Graphene, Nanocarbons for Advanced Energy Storage", Wiley-VCH Verlag GmbH & Co. KGaA2, 211-225, 2015

[8] T. Kim, G. Jung, S. Yoo, K.S. Suh, R.S. "Ruoff, Activated Graphene-Based Carbons as Supercapacitor Electrodes with Macro- and Mesopores", ACS Nano, 7, 6899, 2013.

[9] M. Shanmugam, R. Jayavel, "Synthesize of Graphene-Tin Oxide Nanocomposite and Its Photocatalytic Properties for the Degradation of Organic Pollutants Under Visible Light", J. Nanosci. and Nanotech., 15, 7195, 2015.

[10] X. Liu, L. Pan, T. Lv, Z. Sun, "Investigation of photocatalytic activities over ZnO–TiO_2–reduced graphene oxide composites synthesized via microwave-assisted reaction", J. Colloid Interface Sci., 394, 441, 2013.

[11] G. Jeevitha, R. Abhinayaa, D. Mangalaraj, N. Ponpandian, "Tungsten oxide-graphene oxide (WO_3-GO) nanocomposite as an efficient photocatalyst, antibacterial and anticancer agent", J. Phys. Chem. Solids, 116, 137, 2018.

[12] S. Humaira, K.C. Kemp, C. Vimlesh, S.K. Kwang, "Graphene–SnO_2 composites for highly efficient photocatalytic degradation of methylene blue under sunlight", Nanotechnology, 23, 355705, 2012.

[13] M. Shanmugam, A. Alsalme, A. Alghamdi, R. Jayavel, "In-situ microwave synthesis of graphene–TiO_2 nanocomposites with enhanced photocatalytic properties for the degradation of organic pollutants", J. Photochem. Photobiol., B, 163, 216, 2016.

[14] P. Thakur, R. Chadha, N. Biswas, S.K. Sarkar, T. Mukherjee, S.S. Joshi, S. Kapoor, "Synthesis and characterization of CdS doped TiO_2 nanocrystalline powder: A spectroscopic study", Mater. Res. Bull., 47, 1719, 2012.

[15] J. Fan, S. Liu, J. Yu, "Enhanced photovoltaic performance of dye-sensitized solar cells based on TiO_2 nanosheets/graphene composite films", J. Mater. Chem., 22, 17027, 2012.

[16] J. Guo, Y. Li, S. Zhu, Z. Chen, Q. Liu, D. Zhang, W.-J. Moon, D.-M. Song, "Synthesis of WO_3@Graphene composite for enhanced photocatalytic oxygen evolution from water", RSC Adv., 2, 1356, 2012.

[17] L.-L. Xing, K.-J. Huang, L.-X. Fang, "Preparation of layered graphene and tungsten oxide hybrids for enhanced performance supercapacitors", Dalton Trans., 45, 17439, 2016.

[18] H.-K. Kim, D. Mhamane, M.-S. Kim, H.-K. Roh, V. Aravindan, S. Madhavi, K.C. Roh, K.-B. Kim, "TiO_2-reduced graphene oxide nanocomposites by microwave-assisted forced hydrolysis as excellent insertion anode for Li-ion battery and capacitor", J. Power Sources, 327, 171, 2016.

[19] J. Wang, Z. Gao, Z. Li, B. Wang, Y. Yan, Q. Liu, T. Mann, M. Zhang, Z. Jiang, "Green synthesis of graphene nanosheets/ZnO composites and electrochemical properties", J. Solid State Chem., 184, 1421, 2011.